The Ultra-low Frequency and Broad Band Gaps Characteristics of Multilayer Composite Cylindrical Three-dimensional pentamode metamaterials

Chengxin Cai
Henan University of Technology), Ministry of Education
Xue Wang
Henan University of Technology), Ministry of Education
Qifu Wang
Henan Academy of Science
Mingxing Li
Henan University of Technology), Ministry of Education
Guangchen He
Henan University of Technology), Ministry of Education
Zhaohong Wang
Xi'an Jiaotong University
Qin Yao (eqinyao@163.com)
Henan University of Technology

Research Article

Keywords: pentamode, metamaterials, frequency, ultra, band

Posted Date: October 22nd, 2021

DOI: https://doi.org/10.21203/rs.3.rs-969950/v1

The Ultra-low Frequency and Broad Band Gaps Characteristics of Multilayer Composite Cylindrical Three-dimensional pentamode metamaterials

Chengxin Cai[1,2*], Xue Wang[1], Qifu Wang[3], Mingxing Li[1], Guangchen He[1], Zhaohong Wang[4], Qin Yao[2*]

[1]*Key Laboratory of Grain Information Processing and Control (Henan University of Technology), Ministry of Education, Zhengzhou 450001, China*

[2]*College of Information Science and Engineering, Henan University of Technology, Zhengzhou 450001, China*

[3]*Institute of Applied Physics, Henan Academy of Science, Zhengzhou 450001, People's Republic of China*

[4] *Key Laboratory for Physical Electronics and Devices of the Ministry of Education, Xi'an Jiaotong University, Xi'an 710049, People's Republic of China*

Email: cxcai2018@haut.edu.cn

Abstract: For three-dimensional pentamode metamaterials, it is of great significance to realize underwater ultra-low frequency acoustic wave control. Therefore, two types multilayer composite cylindrical three-dimensional pentamode metamaterials with ultra-low frequency and broad band gaps are proposed in this paper. By using pentamode metamaterials with lattice constants on the order of centimeters, the phononic band gaps below 60 Hz and the single-mode area below 30Hz can be obtained. Compared with asymmetrical double-cone locally resonant pentamode metamaterials, the lower edge frequency, relative bandwidth and figure of merit of the first phononic band gap can be reduced by up to 61.4%, 10.3% and 40.6%, respectively. It will provide reference and guidance for the engineering application of pentamode metamaterials in controlling the ultra-low frequency broadband acoustic waves, vibration and noise reduction.

1.Introduction

The concept of pentamode metamaterials (PMs) was first proposed by Milton and

Cherkaev in 1995[1]. The equivalent elastic properties of PMs can be expressed as in the six-dimensional stress space, only the eigenvalue of the volume compression mode is not zero, and the other five characteristic values of the shear mode are zero. Such a solid structure will show the mechanical properties of traditional fluids as a whole, it is a complex "fluid" with solid characteristics. In theory, the acoustic metamaterials composed of such a periodic arrangement of structural units can achieve a perfect match with water. Therefore, the characteristics of adjustable modulus anisotropy, solid characteristics and wide frequency endow the PMs with excellent sound wave control capabilities, which have important potential applications in the fields of sound wave control, earthquake protection, vibration and noise reduction [2, 4-14].

In 2006, Milton introduced the feasibility of using PMs for elastic wave stealth through the change law of traditional elastic dynamics equations under curve transformation [15]. In 2007, Chen Huanyang *et al.* used the invariance of the direct current conductance equation under coordinate transformation to establish a one-to-one correspondence between the acoustic wave equation and the direct current conductance equation, and derived the general three-dimensional transformation acoustic equation for the first time [16]. In 2008, Norris systematically analyzed the inertial acoustic stealth and the PMs acoustic cloak, and proposed the possibility of applying the transform acoustic theory to the PMs [2]. In 2010, Scandrett *et al.* proposed a method of designing acoustic cloaks using layered PMs [17-18]. In 2012, Kadic *et al.* used laser direct writing technology and artificial additive manufacturing technology to produce three-dimensional PMs samples of micrometer and millimeter order for the first time, and conducted mechanical and acoustic properties research [19, 20]. In 2014, N. Aravations-Zafiris *et al.* designed a three-dimensional layered column structure with pentamode characteristic, which broadened the array structure of PMs units [21]. This has also aroused the interest of researchers in the different lattice configurations of PMs [22]. In 2018, Liu Xiaozhou *et al.* designed a carpet-style PMs acoustic cloak suitable for underwater broad by adjusting the microstructure geometric parameters of the two-dimensional PMs, provided a new choice for PMs in acoustic stealth devices [10]. In 2020, Huang Guoliang *et al.* designed a two-dimensional elastic wave stealth cloak

using the extreme characteristics of similar PMs, which will provide a useful reference for exploring the underwater acoustic wave control of PMs [13-14].

At present, low-frequency detection sonars with operating frequencies below 300 Hz have appeared, which requires PMs to have the ability to control underwater low-frequency sound waves. For the PMs composed of simple materials, they generally belong to the Bragg scattering PMs, and their lattice size is generally the same order of magnitude as the acoustic wavelength corresponding to the operating frequency. If the Bragg scattering PMs is used to control low-frequency sound waves below 300 Hz, the structural size of the sound wave control device needs to be at least tens of meters, which brings great difficulties in engineering application. Therefore, studying the method and mechanism of small-scale PMs to control underwater low-frequency sound waves and establishing a three-dimensional control method for working frequency bands are the core issues that need to be solved urgently.

Generally, the wavelength corresponding to the acoustic/elastic wave phononic band gap (PBG) formed by Bragg scattering is in the same order of magnitude of the lattice constant. Due to the limitation of the lattice size, it is difficult to apply Bragg scattering PMs at low frequencies (especially below 100 Hz). In order to overcome the shortcomings of Bragg scattering PMs, we propose two cylindrical three-dimensional PMs with ultra-low frequency and broad band gaps. The primitive of multilayer composite cylindrical is composed of composite materials, one part provides the quality required by the structural unit, that is, a hard material. The other part provides the elasticity required by the resonance of the structural unit, that is, a soft material. Furthermore, the finite element simulation software COMSOL Multiphysics is used to carry out the numerical analysis of its band structure, single-mode area and pentamodal performance. Furtherly, the effects of asymmetry on the PBG, single-mode area and figure of merit (FOM) of the three samples are discussed. The lower frequency and broad band gaps will endow the structure with better potential for underwater sound wave control.

2.Structure design and energy band characteristics of multilayer composite cylindrical three-dimensional PMs

The unit cell structure of multilayer composite cylindrical three-dimensional PMs is shown in figure 1(a). It consists of 16 primitives connected at the narrow end to form a face-centered cubic structure with a lattice constant of a. Three types primitives are shown in figure 1(b) and composed by two materials. In order to comparative analysis conveniently, we define them as S1, S2 and S3 respectively. For S1, the primitive structure is the composite asymmetric double-cone element. The soft material is at the narrow diameter at both ends (d_1 and d_2), and the length is h_1. For S2, it is one of multilayer composite cylindrical three-dimensional PMs. The soft material is added at both ends, the length is h_1, and the diameters from the top to the bottom of the primitive structure are d_1、D_1、D_3、D_3、D_2、d_2, the heights of the corresponding cylinders are h_1、h_2、h_3、h_3、h_2、h_1, and satisfy the equivalent relationship of h_1+h_2+h_3=1/2H. For S3, the soft material is added to the middle position of the primitive, and the structural parameters are the same as S2. Here, we define the ratio of narrow diameter of soft materials as asymmetry degree

$$\begin{cases} \frac{d_2}{d_1} = N_1 & \text{for S1} \\ \frac{d_2}{d_1} = N_2 & \text{for S2} \\ \frac{d_2}{d_1} = N_3 & \text{for S3} \end{cases} \tag{1}$$

In order to facilitate comparative analysis, the hard and soft materials of three samples are polymers and silicone rubber, respectively. The material parameters are shown in Table1.

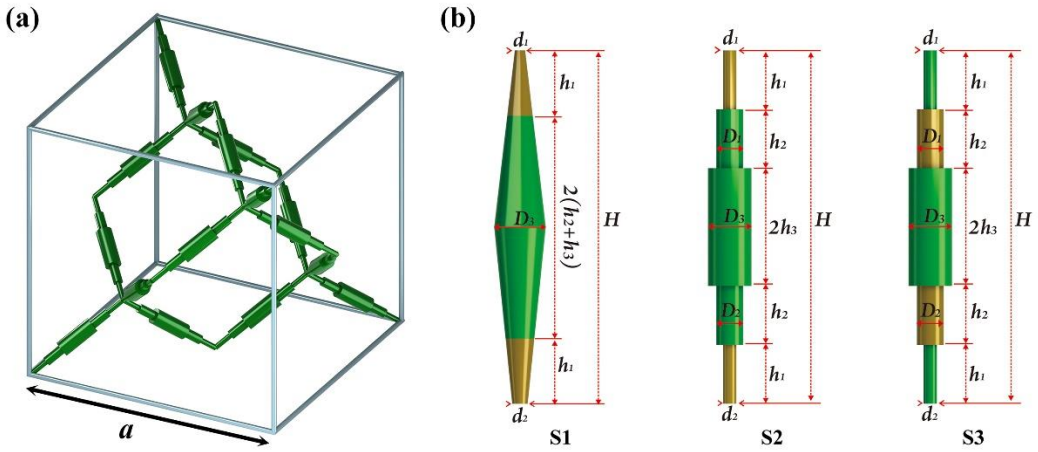

Figure 1. (a) The unit cell structure diagram of the multilayer composite cylindrical three-dimensional PMs. (b) Primitive structure diagrams of three local resonance PMs.

Table 1. Material parameters

Materials	ρ	E	υ
Ploymer	1190 kg/m^3	3Gpa	0.4
Silicon Rubber	1300 kg/m^3	0.1175×10^{-3}	0.47

For calculating the phononic band structure, the Bloch boundary conditions are applied on the primitive unit cells of the three locally resonant PMs in the finite element simulation software COMSOL Multiphysics. The fixed structure parameters are S1: a=37.3mm, H=16.15mm, D =3mm, d_1 =0.55mm, h_1 = 0.1 H. S2: D_3 =3mm, $D_1 = D_2$ =1.5mm, d_1 =0.55mm, h_1 = 0.1 H, h_2 = 0.3 H, h_3 = 0.1 H. S3: D_3=3mm, D_1=1.5mm, d_1=d_2=0.55mm, h_1=0.1H, h_2=0.3H, h_3=0.1H. Select the asymmetry degrees $N_1 = N_2 = N_3$ =0.6 as a reference, and the calculated band structures of the three samples are shown in figure 2.

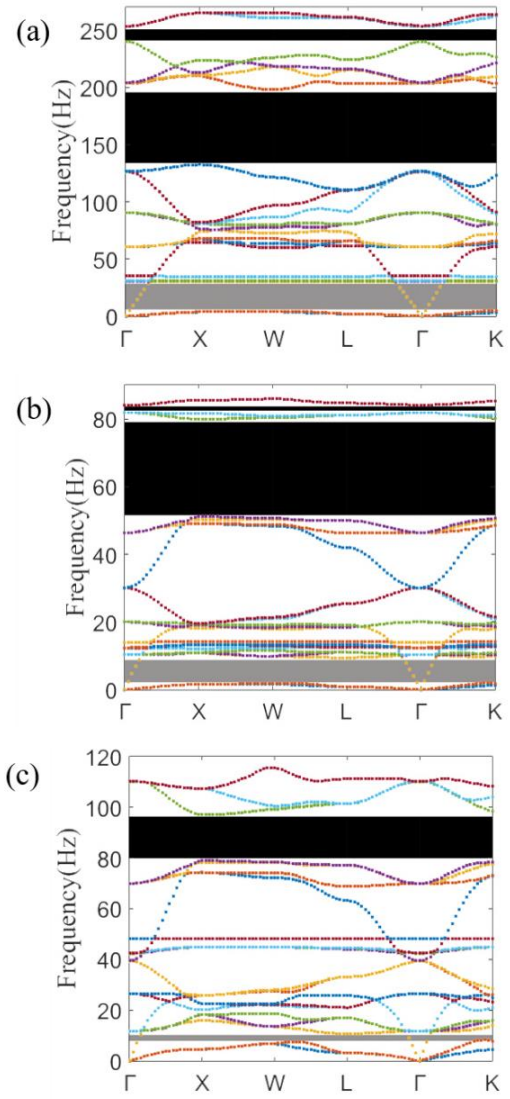

Figure 2. The phononic band structure of locally resonant PMs composed by (a) S1, (b) S2, (c) S3.

The phononic band structure of the S1 is shown in figure 2(a). Not only are there two PBG in the phononic band structure diagram, but also the relatively flat energy bands appear near PBG. These flat energy bands mean the existence of resonance modes. The frequencies of the lower edge (f_l) and upper egde (f_u) of the first PBG are 132.42 Hz and 198.19 Hz, respectively. The relative bandwidth of the first PBG ($\Delta\omega/\omega_g = \frac{\Delta\omega}{(f_u+f_l)/2}$) is 0.398. The lower and upper edge frequencies of the second PBG are 240.06 Hz and 253 Hz, respectively. The relative bandwidth of the second PBG is 0.052. The phononic band structure of the S2 is shown in figure 2(b). It can be seen that two complete PBGs can be opened in addition to the single-mode area. The lower and upper

edge frequencies of the first PBG are 51.16 Hz and 79.95 Hz, respectively. The relative bandwidth of the first PBG is 0.439. The lower and upper edge frequencies of the second PBG are 81.9 Hz and 83.97 Hz, respectively. The relative bandwidth of the second PBG is 0.025. The phononic band structure of the S3 is shown in figure 2(c). It is obvious that there is only one PBG in the phononic band structure diagram. The lower and upper edge frequencies of the first PBG are 78.99 Hz and 97.06 Hz, respectively. The relative bandwidth of the first PBG is 0.205.

To sum up, compared with the asymmetric double-cone locally resonant PMs, the two types multilayer cylindrical locally resonant PMs can not only obtain the complete PBG, also can greatly reduce the frequency of the first PBG. For S2 and S3, they can reduce the lower edge frequency of the first PBGs by 61.4% and 40.3%, respectively. In addition, the bandwidth of the first PBG can be extended, which is 10.3% higher than the relative bandwidth of asymmetric double-cone locally resonant PMs. This means that the using locally resonant PMs formed by S2 to control ultra-low frequency acoustic/elastic waves will produce more excellent effects. However, it is clear that locally resonant PMs formed by S3 are more stable than S2.

3.The influence of asymmetry degrees on the first PBG

The Bragg scattering mechanism emphasizes the influence of periodic structure on waves, while the locally resonant mechanism emphasizes the interaction between the resonance characteristics of the scatterer unit and the waves in the matrix. Since the lower and upper frequencies of the PBG of the locally resonant PMs can be equivalent to the principle of the "spring-mass" system, by analyzing the equivalent parameters in the simplified model, the change trend of the PBG is analyzed. The relationship between the lower edge frequency of the first PBG and the equivalent stiffness k_{sieff} and the equivalent mass M_{sieff} of the three types locally resonant PMs can be expressed in the following proportional relationship:

$$f_{lsi} = \frac{1}{2\pi}\sqrt{\frac{k_{sieff}}{M_{sieff}}} \quad (i=1,2,3) \tag{2}$$

At the same time, the equivalent stiffness k_{sieff} and equivalent mass M_{sieff} of three locally resonant PMs are approximately expressed as [23]:

$$\begin{cases} k_{s1eff} \propto \frac{C_{11}[d_1(H-2h_1)]+2h_1D_3}{Hh_1} & (d_1 < d_2) \\ k_{s1eff} \propto \frac{C_{11}[d_2(H-2h_1)]+2h_1D_3}{Hh_1} & (d_2 < d_1) \\ M_{s1eff} = m_2 + m_3 + m_4 & (d_1 < d_2) \\ M_{s1eff} = m_1 + m_2 + m_3 & (d_2 < d_1) \end{cases}$$ for S1 (3)

$$\begin{cases} k_{s2eff} \propto \frac{C_{11}({d_1}^2+{d_2}^2)}{h_1} \\ M_{s2eff} = m_2 + m_3 + m_4 + m_5 \end{cases}$$ for S2 (4)

$$\begin{cases} k_{s3eff} \propto \frac{C_{11}({D_1}^2+{D_2}^2)}{h_1} \\ M_{s3eff} = m_2 + m_3 + m_4 + \alpha_1 m_5 + m_6 & (D_1 < D_2) \\ M_{s3eff} = m_1 + m_3 + m_4 + m_6 + \alpha_2(m_2 + m_5) & (D_2 < D_1) \\ 0 < \alpha_1 < 1, 0 < \alpha_2 < 1 \end{cases}$$

for S3 (5)

Where $C_{11} = \lambda_{silicone\ rubber} + 2\mu_{silicone\ rubber}$, $\lambda_{silicone\ rubber} = 6 \times 10^{-4} GPa$, $\mu_{silicone\ rubber} = 4 \times 10^{-5} GPa$, α_1 and α_2 are the undeformed coefficients at the position where the soft material is added.

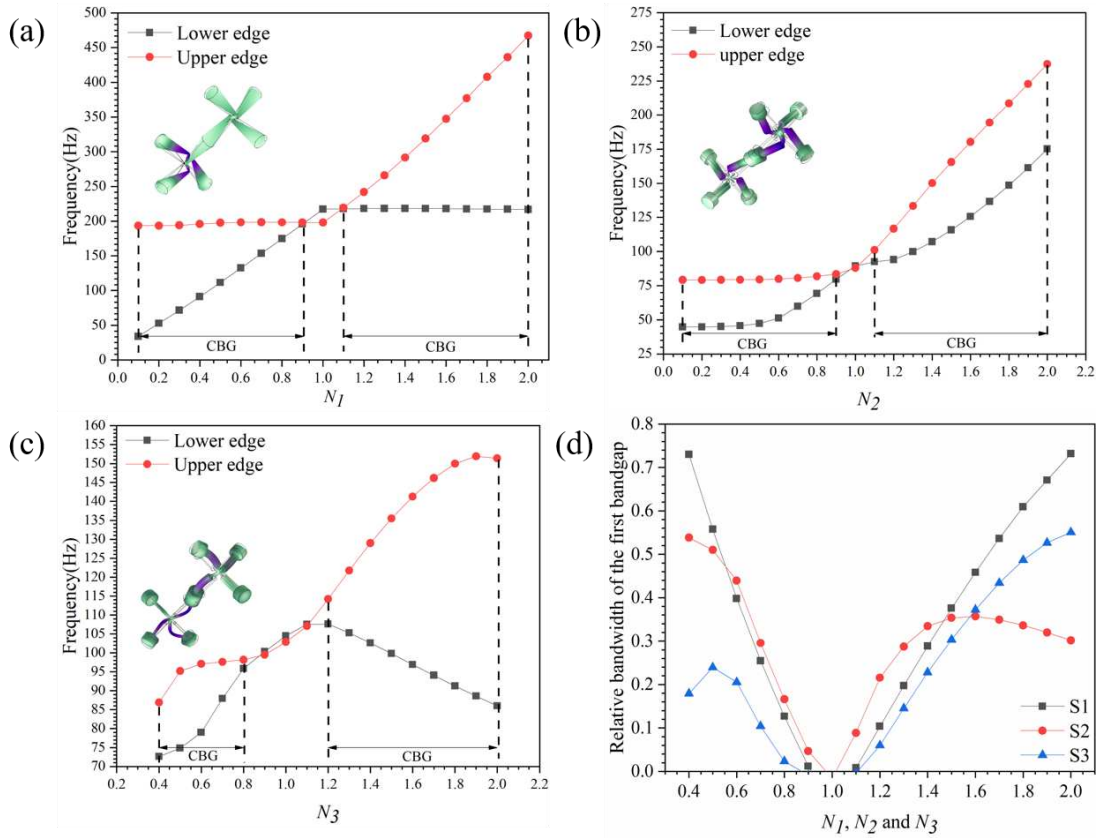

Figure 3. The influence of N_1、N_2、N_3 on the PBG of (a) S1, (b) S2 And (c) S3. (d) Comparison of the influence of asymmetry degrees on the relative bandwidth of the

first PBG of three samples (S1, S2, S3).

Any structural parameter that can cause changes in the equivalent parameters of the locally resonant will have an impact on the lower and upper frequencies of the first PBGs. In order to further study the locally resonant characteristics of the three samples, the influence of the asymmetry degrees (N_1, N_2, and N_3)on the first PBG and relative bandwidth was studied and some results were shown in figure 3.

The influence of N_1 on the first PBGs of S1 was shown in figure 3(a), and the vibration mode of the lower edge frequency of the first band gap is given when N_1=0.4. It can be seen that when N_1 ranges from 0.1 to 0.9, d_2 is more easily to deform. With the increase of N_1, the narrow diameter d_2 increases, the equivalent stiffness k_{s1eff} produced by its deformation also is increased, while the change of the equivalent mass M_{s1eff} is negligible, so the lower edge frequency of first PBG increases with increase of N_1. When N_1 ranges from 1.1 to 2.0, d_1 is more easily to deform. At this time, the lower edge frequency of the first PBG is mainly determined by the equivalent stiffness k_{s1eff} produced by the deformation of d_1, while d_1 is a fixed parameter, which basically remains constant. Therefore, the lower edge frequency of the first PBG is basically unchanged.

The influence of N_2 on the first PBGs of S2 was shown in figure 3(b), and the vibration mode of the lower edge frequency of the first band gap is given when N_2=0.4. When N_2 changes from 0.1 to 2.0, the equivalent stiffness k_{s2eff} is determined by both d_1 and d_2 due to the deformation at both d_1 and d_2. With the increase of N_2, the equivalent stiffness k_{s2eff} also increases, while the equivalent mass M_{s2eff} remains basically unchanged, so the lower edge frequency of the first PBG increases with the increase of N_2.

The influence of N_3 on the first PBGs of S3 was shown in figure 3(c), and the vibration mode of the lower edge frequency of the first band gap is given when N_3=0.4. When N_3 changes from 0.1 to 1.0, the equivalent stiffness k_{s3eff} generated by the deformation at d_1 and d_2 increases at the same time, so the lower edge frequency of the first PBG gradually increases with the increase of N_3. When N_3 changes from 1.1 to 2.0, as d_1 and d_2 continue to increase, the deformation part of the soft material

becomes smaller, and the part that does not deform increases, which causes the equivalent mass M_{s3eff} increases. At the same time, since the equivalent stiffness k_{s3eff} decreases, the lower edge frequency of the first PBG shows a downward trend as N_3 increases.

Figure 3(d) shows the influence of asymmetry degrees on the relative bandwidth of the first PBG of the three samples (S1, S2, S3). When the asymmetry degrees change in the range of 0.6 to 1.4, the relative bandwidth of the S2 is significantly higher than that of the S1. In addition, when N_1 and N_2 change in the range of 0.6 to 1.4, the lower edge frequency of the first PBG of S1 increased from 91.1 Hz to 218.12 Hz, while the lower edge frequency of the first PBG of S2 increased from 51.16 Hz to 107.2 Hz. Therefore, compared with the S1 type locally PMs, the S2 type locally PMs can not only reduce the lower edge frequency of the first PBG by 43.8% to 50.9%, but also broaden the relative bandwidth of the first PBG.

4.Single-mode region

The single-mode area is the frequency region that limits the decoupling of compression waves and shear waves, and it is an important factor to measure the pentamode characters of locally PMs, Therefore, it is necessary to further study the single-mode performance of the three samples. Figure 4 shows the effects of asymmetry degrees N_1, N_2, and N_3 on the upper and lower edge frequencies and relative bandwidths of the single-mode regions of the three samples. Obviously, the single-mode lower edge frequency of S1 and S2 increases slowly with the increase of asymmetry, and S3 shows a trend of first rising and then decreasing slightly with the increase of asymmetry. Among them, the single-mode lower edge frequency corresponding to S1 is the lowest. With the increase of asymmetry, the single-mode upper edge frequency of S1 and S2 showed a sharp increase and a gentle increase trend, respectively, while S3 first slowly increased and then decreased slightly. Therefore, the relative bandwidth of the single-mode area of the S1 is the largest, which is basically maintained at about 1.46. while S2 is second, showing a trend of first rising and then decreasing. The relative bandwidth of the single-mode area of S3 gradually increases

with the increase of asymmetry N_3, and reaches the maximum value of 0.95 when N_3 is equal to 2.0.

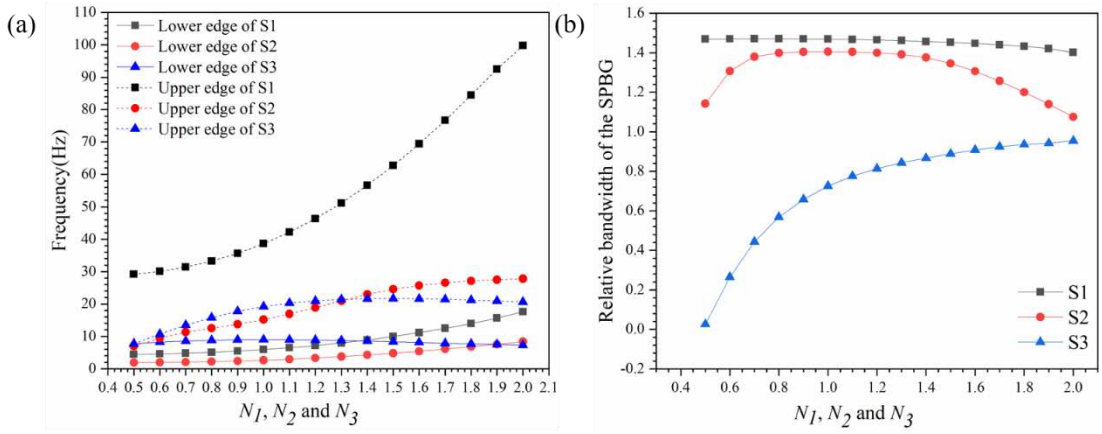

Figure 4. The influence of asymmetry degrees N_1, N_2, N_3 on the (a) bandwidth and (b) relative bandwidth of the single-mode area.

5.Pentamodal performance

The FOM is defined as the ratio of the equivalent bulk modulus (B) to the equivalent shear modulus (G). The larger the FOM, the easier it is to decouple the compression and shear waves, thereby obtaining good pentamodal performance. The FOM has the following proportional relationship with the ratio of compression and shear waves phase velocity:

$$\text{FOM}=\frac{B}{G} \propto \left(\frac{C_B}{C_G}\right)^2 \tag{6}$$

While, the compression wave phase velocity (C_B) and shear wave phase velocity (C_G) of locally resonant PMs are determined by the slope of the compression and shear waves of phononic band.

Figure 5 shows the influence of asymmetry degrees on the FOM of three samples. Both S1 and S2 showed a trend of first increasing and then decreasing with the increase of asymmetry degrees. The FOM of S1 reached the maximum value of 514.29 when N_1=0.9, and the FOM of S2 reached the maximum value of 723.1 when N_2=0.8. For S3, it increases slowly with the increase of N_3, and FOM reaches the maximum value of 97.05 when N_3=2.0. The above analysis shows that, compared with S1, the FOM of S2 can be increased by up to 40.6%.

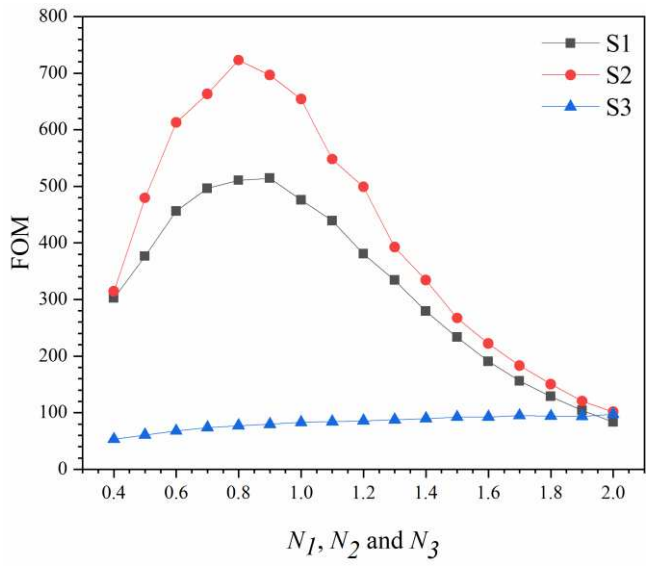

Figure 5. The influence of asymmetry degrees on FOM of the three samples.

6.Conclusion

For Bragg scattering PMs, using the PMs to achieve underwater sound insulation below 100Hz requires a material with a several meters thick lattice size. In this paper, two types multilayer composite cylindrical three-dimensional PMs are proposed. In order to compare and analyze with the asymmetrical double-cone locally resonant PMs, a large number of numerical calculations have been carried out on the influence of asymmetry N_1, N_2, N_3 on the phononic band gap, single-mode area, and FOM of the three samples (S1, S2, S3). Numerical results show that compared with S1 type locally resonant PMs, S2 type locally resonant PMs proposed in this paper can reduce the lower edge frequency of the first PBG by up to 61.4%, increase the relative bandwidth of the first PBG by up to 10.3%, and increase the FOM by up to 40.6%. This research will provide a theoretical basis and reference for further promoting the application of three-dimensional PMs in underwater low-frequency acoustic wave control devices.

Acknowledgements

The research has been partially supported by the National Nature Science Foundations of China (Grant No. 52003076), Key Laboratory of Grain Information Processing and Control of Ministry of Education (Grant Nos. KFJJ-2020-106 and KFJJ-2018-102), High-level Talent Fund of Henan University of Technology (Grant Nos. 31401120 and 31401232), Cultivation Plan for Young Key Teachers of Higher Education Institutions in Henan Province

(2021GGJS065) and Cultivation Program for Young Backbone Teachers in Henan University of Technology.

References

[1] Milton G W, Cherkaev A V. Which elasticity tensors are realizable? *Journal of Engineering Materials and Technology*, **117**: 483-493(1995).

[2] Norris A N. Acoustic cloaking theory. *Proceedings of the Royal Society A: Mathematical, Physical and Engineering Sciences*, **464**: 2411-2434 (2008).

[3] Sun Z Y, Jia H, Chen Y, Wang Z, Yang J. Design of an underwater acoustic bend by pentamode metafluid. *The Journal of the Acoustical Society of America*, **143**: 1029 (2018).

[4] Chen Y, Liu X N, Hu G K. Latticed pentamode acoustic cloak. *Scientific Reports*, **5**: 15745 (2015).

[5] Xiao Q J, Wang L, Wu T, Zhao Z G. 2014. Research on layered design of ring-shaped acoustic cloaking using bimode metamaterial. *Applied Mechanics and Materials*, **687-691**:4399-4404 (2014).

[6] Zhao A G, Zhao Z G, Zhang X D. Cai X, Wang L, Wu T, Chen H. Design and experimental verification of a water-like pentamode material. *Applied Physics Letters*, **110**: 011907 (2017).

[7] Chen Y, Liu X N, Hu G K. Design of arbitrary shaped pentamode acoustic cloak based on quasi-symmetric mapping gradient algorithm. *The Journal of the Acoustical Society of America*, **140** (5): EL405-EL409 (2016).

[8] Chen Y, Zheng M Y, Liu X N, Bi Y F, Sun Z Y, Xiang P, Yang J, Hu G K. Broad solid cloak for underwater acoustics. *Physical Review B*, **95**: 180104 (2017).

[9] Lu Z M, Cai L, Wen J H, Wen X S. Research on coordinate transformation design of a cylinderical acoustic cloak with pentamode materials. *Acta Physica Sinica*, **65**: 174301 (2016).

[10] Chen J G, Liu J H, Liu X Z. Broad underwater acoustic carpet cloak based on pentamode materials under normal incidence. *AIP Advance*, **8**:085024 (2018).

[11] Su X S, Norris A N, Cushing C W, Haberman M R, Wilson P S. Broad focusing of

underwater sound using a transparent pentamode lens. *The Journal of the Acoustical Society of America*, **141** (6) (2017).

[12] Chen Y, Hu G K. Broad and high-transmission metasurface for converting underwater cylindrical waves to plane waves. *Physical Review Applied*, **12**:004046 (2019).

[13] Xu X C, *et al*. Physical Realization of elastic cloaking with a polar material. *Physical Review Letters*, **124**: 114301 (2020).

[14] Nassar H, Chen Y Y, Huang G L. Polar metamaterials: a new outlook on resonance for cloaking applications. *Physical Review Letters*, **124**: 084301 (2020).

[15] Milton G W, Briane M, Willis J R. On cloaking for elasticity and physical equations with a transformation invariant form. *New Journal of Physics*, **8**: 248 (2006).

[16] Chen H Y, Chan C T. Acoustic cloaking in three dimensions using acoustic metamaterials. *Applied Physics Letter*s, **91**(18):183518 (2007).

[17] Scandrett C L, Boisvert J E, Howarth T R. Acoustic cloaking using layered pentamode materials. *The Journal of the Acoustical Society of America*, **127**: 2856-2864 (2010).

[18] Scandrett C L, Boisvert J E, Howarth T R. Broad optimization of a pentamode-layered spherical acoustic waveguide. *Wave Motion*, **48**: 505-514 (2011).

[19] Martin A, Kadic M, Schittny R, BÄuckmann T, Wegener M. Phonon band structures of three-dimensional pentamode metamaterials. *Physical Review B*, **86**: 155116 (2012).

[20] Kadic M, BÄuckmann T, Stenger N, Thiel M, Wegener M. On the practicability of pentamode mechanical metamaterials. *Applied Physics Letters*, **100**: 191901 (2012).

[21] Aravantinos-Zafiris N, Sigalas M M, Economou E N. Elastodynamic behavior of the three dimensional layer-by-layer metamaterial structure. *Journal of Applied Physics*, **116**(13):133503 (2014).

[22] Huang Y, Lu X G, Liang G Y, Xu Z. Comparative study of the pentamodal property of four potential pentamode microstructures. *Journal of Applied Physics*, **121**:125110 (2017).

[23] Cai C X, Han C, Wu J F, Wang Z H, Zhang Q H. Tuning method of phononic band

gaps of locally resonant pentamode metamaterials. *Journal of Physics D: Applied Physics*, **52**: 045601 (2019).